CORRELATIONS WITH FLUCTUATING STRINGS* **

Wojciech Broniowski[a,b,†], Martin Rohrmoser[a,‡]

[a]Institute of Physics, Jan Kochanowski University, 25-406 Kielce, Poland
[b]Institute of Nuclear Physics Polish Academy of Sciences, 31-342 Kraków, Poland

We present a semi-analytic approach to the forward–backward multiplicity correlations in ultra-relativistic nuclear collisions, based on particle emission from strings with fluctuating end-points. We show that with the constraints from rapidity spectra, one can obtain bounds for the magnitude of the standard measures of the forward–backward fluctuations. The method is generic under the assumption of independent production from sources. For definiteness, we use the wounded quark model for Au+Au and d+Au collisions at the energy of $\sqrt{s_{NN}} = 200$ GeV.

This paper is based on our recent work [1], where more details may be found. Our primary goal is to understand in simple terms the mechanism of generation of the forward–backward multiplicity fluctuations in ultra-relativistic nuclear collisions. The presented approach generalizes in a natural way the analysis of [2], where only one-end fluctuations of strings were incorporated.

The QCD-motivated string models are being used all over the particle physics phenomenology. In particular, numerous and successful Monte Carlo codes are based on the Lund model of the string formation and decay (see, *e.g.*, [3–8]), or on the Dual Parton Model involving Pomeron and Regge exchange [9–11]. A shared feature is the formation of a collection of strings in the early stage of the collision. The string end-points span the color field and have opposite color charges (triplet with the quark–diquark or

quark–antiquark, or octet with the gluon–gluon strings). The location of the end-points in spatial rapidity fluctuates randomly according to appropriate parton distribution functions, which together with other incorporated effects (such as the nuclear shadowing or baryon stopping) leads to predictions of the one-body spectra and the forward–backward event-by-event fluctuations.

On the other hand, multiplicity in hadron production is successfully described within the wounded picture [12], where the Glauber model [13] is adopted to describe inelastic collisions [14]. It has been found that the scaling based on wounded quarks [15–18] rather than nucleons works surprisingly well [19–35] at RHIC and the LHC.

The approach of [1, 2] used here merges the two above concepts in the following manner:

1. Each wounded quark pulls a string;

2. The end-points of the strings are generated from appropriate distributions in such a way that the experimental one-body pseudorapidity spectra, serving as a constraint, are reproduced;

3. The emission of particles from a string between its end-points is uniform in space-time rapidity;

4. The strings emit particles independently of one another;

5. For clarity, we consider only one type of strings, which leads to a simple semi-analytic analysis.

Modeling the rapidity spectra in the adopted approach is based on the key formula holding in the nucleon–nucleon (NN) center-of-mass frame (CM)

$$\frac{\mathrm{d}N}{\mathrm{d}\eta} = \langle N_A \rangle f(\eta) + \langle N_B \rangle f(-\eta) \,, \tag{1}$$

where at a given collision energy, $f(\eta)$ should be a universal (*i.e.*, independent of the number of participants) emission profile of a string pulled by a wounded quark (we use the convention that nucleus A moves to the right and B to the left). Whereas from symmetric collisions ($A = B$), one can only obtain the symmetric part of $f(\eta)$, as then $\langle N_A \rangle = \langle N_B \rangle$, from asymmetric collisions, one can also extract the antisymmetric component [36–38]. It has been found that $f(\eta)$ is a widely spread function in essentially the whole available range of η, with a broad peak in the forward direction. A simplified triangular shape of $f(\eta)$ has been used in several works [39–43].

We use the original method of [36] (recently applied also to the wounded quarks [37]) to extract $f(\eta)$ of Eq. (1) from the PHOBOS experimental data [44–46]. The needed valence quark multiplicities $\langle N_A \rangle$ and $\langle N_B \rangle$ in the specified centrality classes were obtained from GLISSANDO [47]. We note

that the results for various centrality classes basically overlap within the experimental uncertainties, hence, we may conclude that the approach yields a universal profile function $f(\eta)$ which reproduces the PHOBOS rapidity spectra at $\sqrt{s_{NN}} = 200$ GeV. We thus confirm the results of [37].

From the point of view of QCD, the roughly triangular shape of $f(\eta)$ seen in Fig. 1 finds its motivation in string models, where one end-point of the string is associated to a valence parton, whereas the other one is randomly generated along the space-time rapidity and is associated to a wee parton [48]. Note that linking the string to a leading (wounded) parton is very much in the spirit of the Lund model [3]. We thus have in each event N_A and N_B "wounded strings" associated to wounded valence quarks in nuclei A and B.
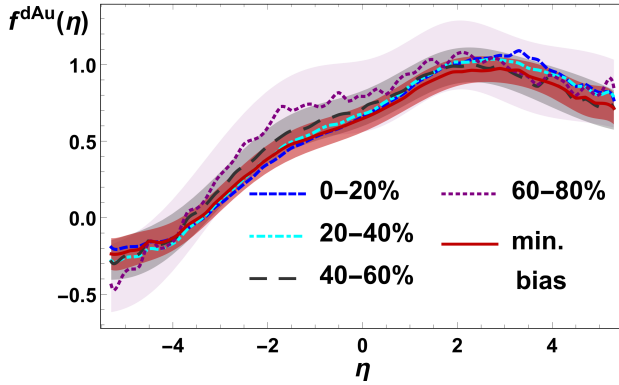

Fig. 1. Emission profiles of strings pulled by the wounded quarks, obtained from fits to the pseudorapidity spectra in d–Au collisions at $\sqrt{s_{NN}} = 200$ GeV from the PHOBOS Collaboration [44, 45]. The bands indicate the experimental uncertainties.

Next, following our recent work [1], we show how the end-point fluctuations relate to the emission profile. Let the emission of a particle with pseudorapidity η from the string fragmentation process be uniformly distributed along the string between its end-points at y_1 and y_2. Then the emission probability distribution is

$$s(\eta; y_1, y_2) = \omega \left[\theta(y_1 < \eta < y_2) + \theta(y_2 < \eta < y_1) \right] , \qquad (2)$$

where ω is the production rate. After a short calculation, we find that

$$f(\eta) = \int\limits_{-\infty}^{\infty} \mathrm{d}y_1 \, g_1(y_1) \int\limits_{-\infty}^{\infty} \mathrm{d}y_2 \, g_2(y_2) s(\eta, y_1, y_2) = \omega \left[\frac{1}{2} - 2H_1(\eta)H_2(\eta) \right] , \quad (3)$$

with the shifted cumulative distribution function defined as

$$H_i(\eta) = G_i(\eta) - \frac{1}{2}, \qquad G_i(\eta) = \int\limits_{-\infty}^{\eta} dy \, g_i(y), \qquad i = 1, 2, \qquad (4)$$

where $G_i(\eta)$ are the standard cumulative distribution functions (CDFs) of the string-end points. Of course, $g_i(\eta) = dG_i(\eta)/d\eta = dH_i(\eta)/d\eta$.

It is clear from Eq. (3) that the procedure of extracting $H_1(\eta)$ and $H_2(\eta)$ when $f(\eta)$ is known is not unique, as the product of two unknown functions is related to a known function. Nevertheless, we will show that interesting bounds may be determined in the considered mathematical problem, since $H_1(\eta)$ and $H_2(\eta)$ are monotonic, continuous, and grow from $-\frac{1}{2}$ to $\frac{1}{2}$ as η increases in its domain. Thus, far to the left, where $H_1(\eta) = H_2(\eta) = -\frac{1}{2}$, and far to the right, where $H_1(\eta) = H_2(\eta) = \frac{1}{2}$, we have $f(\eta) = 0$, as it should be. In between, there must exist somewhere the zeros $\eta_0^{(1)}$ and $\eta_0^{(2)}$ of $H_1(\eta)$ and $H_2(\eta)$, respectively. At these special points, as immediately follows from Eq. (3), $f(\eta_0^{(i)}) = \frac{1}{2}\omega$, which is also the lowest possible value for the maximum of $f(\eta)$. We make a technical assumption here that $f(\eta)$ is unimodal, *i.e.*, has a single maximum at $\eta_{\max}$ (this assumption is justified phenomenologically by the PHOBOS data). The situation where $f(\eta_{\max}) = \frac{1}{2}\omega$ corresponds to the special case $\eta_0^{(1)} = \eta_0^{(2)} = \eta_{\max}$, where we can assume equal distributions for the two end-points

$$H_1(\eta) = H_2(\eta) = \sqrt{\frac{1}{4} - \frac{1}{2\omega} f(\eta)} \, \mathrm{sgn}(\eta - \eta_{\max}). \qquad (5)$$

We label this case "$g_1 = g_2$".

On the other hand, when the maximum of $f(\eta)$ is ω (the highest possible value, assumed when $H_1(\eta_{\max}) = -H_2(\eta_{\max}) = -\frac{1}{2}$), one may choose

$$H_1(\eta) = -\frac{1}{2}\theta(\eta_{\max} - \eta) + \left[\frac{1}{2} - \frac{1}{\omega}f(\eta)\right]\theta(\eta - \eta_{\max}),$$

$$H_2(\eta) = -\left[\frac{1}{2} - \frac{1}{\omega}f(\eta)\right]\theta(\eta_{\max} - \eta) + \frac{1}{2}\theta(\eta - \eta_{\max}). \qquad (6)$$

The supports of $g_1(\eta)$ and $g_2(\eta)$ are disjoint, since H_1 is flat for $\eta < \eta_{\max}$ and H_2 is flat for $\eta > \eta_{\max}$. Thus, we term this case "disjoint".

Finally, there are intermediate cases for $\omega/2 < f(\eta_{\max}) < \omega$. For instance, one may take a given form of $H_1(\eta)$ and then adjust $H_2(\eta)$ to satisfy Eq. (3), namely

$$H_2(\eta) = \frac{\frac{1}{4} - \frac{1}{2\omega}f(\eta)}{H_1(\eta)}. \qquad (7)$$

As $-\frac{1}{2} \leq H_1(\eta) \leq \frac{1}{2}$, flipping the sign at $\eta_0^{(1)}$, Eq. (7) yields

$$
\begin{aligned}
H_2(\eta) &\geq \frac{1}{2} - \frac{1}{\omega} f(\eta) \quad \text{for} \quad \eta \geq \eta_0^{(1)}, \\
H_2(\eta) &\leq -\frac{1}{2} + \frac{1}{\omega} f(\eta) \quad \text{for} \quad \eta \leq \eta_0^{(1)}
\end{aligned}
\tag{8}
$$

(and symmetrically for H_1), hence formulas (6) give the upper and lower bounds for any solution.

Figure 2 presents the distributions of the string end-points and the corresponding CDFs for the three cases: $g_1 = g_2$, disjoint, and intermediate, where one end-point is distributed according to a suitable valence quark distribution function [1]. The bands provide uncertainties propagated from the experimental errors. For $g_1 = g_2$ (single solid line), the distribution peaks at forward rapidity (*i.e.*, the Au side), as expected from the shape of the one-body profile $f(\eta)$ in Fig. 1. In the disjoint case (pairs of dashed lines), the supports for g_1 and g_2 are separated. In the intermediate case, the dotted curve corresponds to the valence quark. It is peaked in the forward
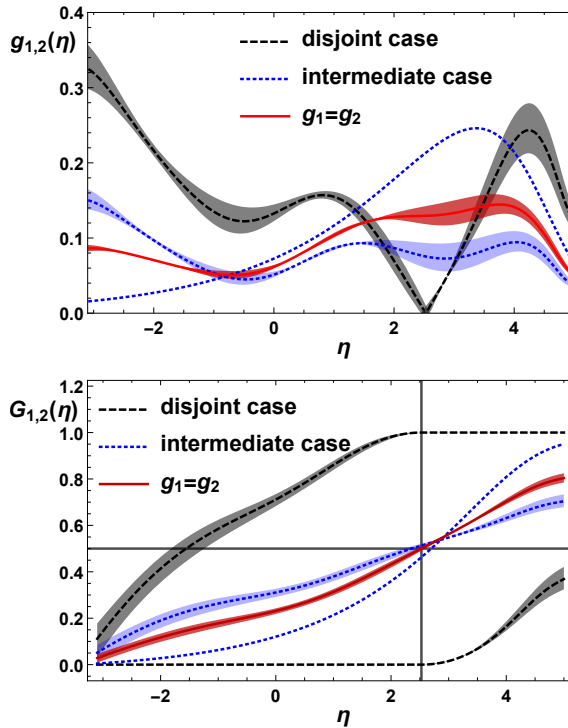

Fig. 2. The end-point probability distribution functions g_1 and g_2 (top) and the corresponding cumulative distribution functions G_1 and G_2 (bottom) for various possibilities described in the text. The vertical line is placed at $\eta_{\max}$.

direction, as expected. With the used parametrization of the valence quark distribution [1], the intermediate case is not far from the $g_1 = g_2$ case. We have verified that this holds for other parameterizations of the valence quark parton distribution functions. We remark that all the substantially different cases of Fig. 2 reproduce by construction the "experimental" emission profile $f(\eta)$.

We are ready to pass to the two-particle distributions, which is the main subject of this paper. We have now for the two-body probability distribution the formula [1]

$$f_2(\eta_1, \eta_2) = \omega^2 G_1[\min(\eta_1, \eta_2)] \{1 - G_2[\max(\eta_1, \eta_2)]\} + (1 \leftrightarrow 2). \quad (9)$$

The covariance of the emission from a single string is defined in a standard way as

$$\mathrm{cov}(\eta_1, \eta_2) = f_2(\eta_1, \eta_2) - f(\eta_1)f(\eta_2). \quad (10)$$

It is displayed in Fig. 3 for the disjoint and $g_1 = g_2$ cases, which are widely different in shape as well as in magnitude, with the former significantly smaller than the latter. The covariance in the intermediate case (not shown) is very close to the $g_1 = g_2$ case.
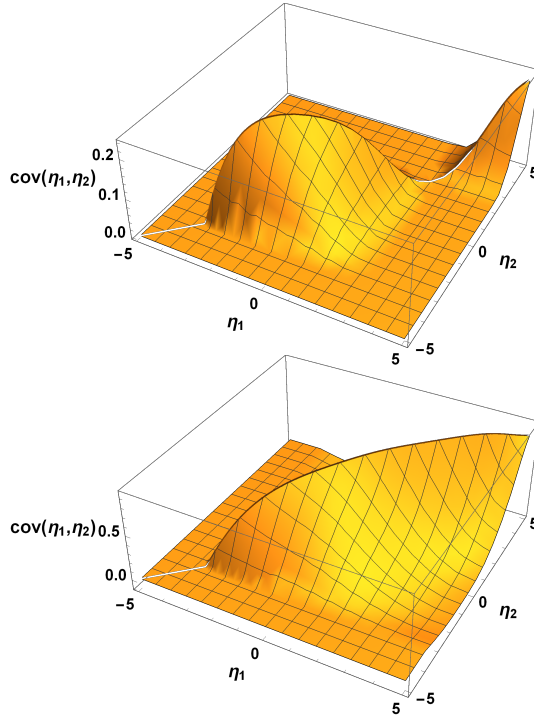

Fig. 3. Covariance of the emission from a single string for the disjoint (top) and $g_1 = g_2$ (bottom) cases.

In a nuclear collision, a collection of strings is formed; they "belong" either to the valence quarks from nucleus A or B. With the key assumption of independent emission from different strings, the expressions for the one- and two-body distributions account for simple combinatorics. For the one-body density in A–B collisions, one has for the whole system (*cf.* Eq. (1))

$$f_{AB}(\eta) = \langle N_A \rangle f_A(\eta) + \langle N_B \rangle f_B(\eta), \tag{11}$$

where $f_A(\eta) = f(\eta)$ and $f_B(\eta) = f(-\eta)$, as A moves forward and B backward in the NN CM frame. Analogously,

$$\begin{aligned}
\mathrm{cov}_{AB}(\eta_1, \eta_2) =\ & \langle N_A \rangle \mathrm{cov}_A(\eta_1, \eta_2) + \langle N_B \rangle \mathrm{cov}_B(\eta_1, \eta_2) \\
& + \mathrm{var}(N_A) f_A(\eta_1) f_A(\eta_2) + \mathrm{var}(N_B) f_B(\eta_1) f_B(\eta_2) \\
& + \mathrm{cov}(N_A, N_B) \left[f_A(\eta_1) f_B(\eta_2) + f_B(\eta_1) f_A(\eta_2) \right].
\end{aligned} \tag{12}$$

We also introduce the customary correlation C defined as

$$C_{AB}(\eta_1, \eta_2) = 1 + \frac{\mathrm{cov}_{AB}(\eta_1, \eta_2)}{f_{AB}(\eta_1) f_{AB}(\eta_2)}, \tag{13}$$

and the a_{nm} coefficients [49–51]

$$a_{nm} = \frac{\int_{-Y}^{Y} \mathrm{d}\eta_1 \int_{-Y}^{Y} \mathrm{d}\eta_2 C(\eta_1, \eta_2) T_n\left(\frac{\eta_1}{Y}\right) T_m\left(\frac{\eta_2}{Y}\right)}{\int_{-Y}^{Y} \mathrm{d}\eta_1 \int_{-Y}^{Y} \mathrm{d}\eta_2 C(\eta_1, \eta_2)}. \tag{14}$$

Here, $[-Y, Y]$ denotes the covered pseudorapidity range, where for RHIC we use $Y = 1$, whereas $T_n(x) = \sqrt{n + 1/2} P_n(x)$ ($P_n(x)$ denote the Legendre polynomials).

Equation (12) contains terms with two different kinds of fluctuations: those originating from the string end-point fluctuations, with $\mathrm{cov}_i(\eta_1, \eta_2)$, and terms with moments of fluctuations of the numbers of wounded quarks, N_A and N_B. We have found that the string end-point fluctuations largely dominate over the N_A and N_B fluctuations, which contribute to a_{11} at the level of 10–20% only.

Figure 4 presents the predicted a_{11} for Au–Au and d–Au collisions at $\sqrt{s_{NN}} = 200$ GeV. We note that the results for the $g_1 = g_2$ and for the intermediate cases are nearly identical, while the result for the disjoint case is about a factor of 3 smaller. In view of the previous discussion, the $g_1 = g_2$ and the disjoint cases represent the upper and lower bounds. From Eq. (12), it is clear that to a good approximation a_{11} scales, as expected, with the inverse of the number of sources.
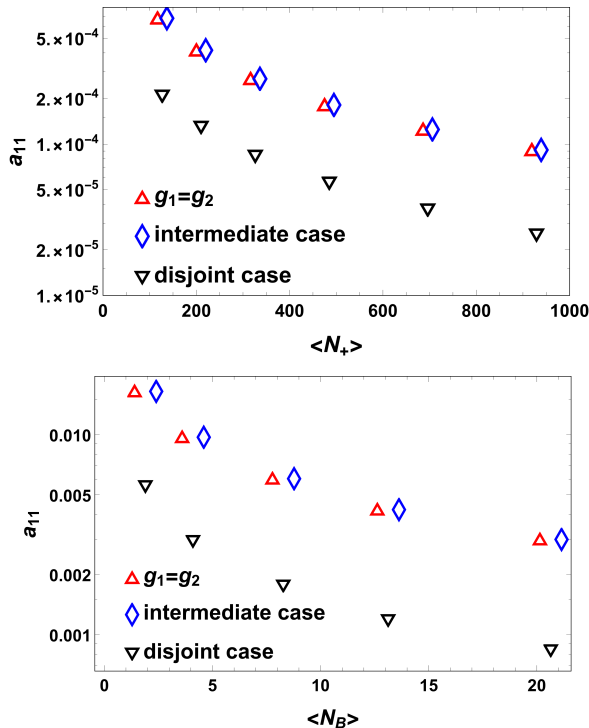
Fig. 4. The predicted a_{11} coefficients for Au–Au (top) and d–Au (bottom) collisions at $\sqrt{s_{NN}} = 200$ GeV, plotted as functions of $N_+ = \langle N_A + N_B \rangle$ or $\langle N_B \rangle$, respectively.

In summary, here are our main points:

— Semi-analytic approach to the analysis of two-body correlations with constraint from the one-body pseudorapidity spectra yields nontrivial bounds for the forward–backward correlation measures;

— Fluctuations of the string end-points yield much larger forward–backward correlations and dominate over fluctuations of the number of strings;

— The a_{nm} Legendre coefficients scale as the inverse of the number of sources (strings).

REFERENCES

[1] M. Rohrmoser, W. Broniowski, *Phys. Rev. C* **99**, 024904 (2019) [arXiv:1809.08666 [nucl-th]].

[2] W. Broniowski, P. Bożek, *Phys. Rev. C* **93**, 064910 (2016) [arXiv:1512.01945 [nucl-th]].

[3] B. Andersson, G. Gustafson, G. Ingelman, T. Sjöstrand, *Phys. Rep.* **97**, 31 (1983).

[4] X.-N. Wang, M. Gyulassy, *Phys. Rev. D* **44**, 3501 (1991).

[5] Z.-W. Lin *et al.*, *Phys. Rev. C* **72**, 064901 (2005) [`arXiv:nucl-th/0411110`].

[6] T. Sjöstrand *et al.*, *Comput. Phys. Commun.* **191**, 159 (2015)
[`arXiv:1410.3012 [hep-ph]`].

[7] C. Bierlich, G. Gustafson, L. Lönnblad, H. Shah, *J. High Energy Phys.*
1810, 134 (2018) [`arXiv:1806.10820 [hep-ph]`].

[8] S. Ferreres-Solé, T. Sjöstrand, *Eur. Phys. J. C* **78**, 983 (2018)
[`arXiv:1808.04619 [hep-ph]`].

[9] A. Capella, U. Sukhatme, C.-I. Tan, J. Tran Thanh Van, *Phys. Rep.* **236**,
225 (1994).

[10] K. Werner *et al.*, *Phys. Rev. C* **82**, 044904 (2010)
[`arXiv:1004.0805 [nucl-th]`].

[11] T. Pierog *et al.*, *Phys. Rev. C* **92**, 034906 (2015)
[`arXiv:1306.0121 [hep-ph]`].

[12] A. Białas, M. Błeszyński, W. Czyż, *Nucl. Phys. B* **111**, 461 (1976).

[13] R.J. Glauber, in: *Lectures in Theoretical Physics*, W.E. Brittin,
L.G. Dunham (Eds.), Interscience, New York 1959, Vol. 1, p. 315.

[14] W. Czyż, L.C. Maximon, *Ann. Phys.* **52**, 59 (1969).

[15] A. Białas, W. Czyż, W. Furmański, *Acta Phys. Pol. B* **8**, 585 (1977).

[16] A. Białas, K. Fiałkowski, W. Słomiński, M. Zieliński, *Acta Phys. Pol. B* **8**,
855 (1977).

[17] A. Białas, W. Czyż, *Acta Phys. Pol. B* **10**, 831 (1979).

[18] V.V. Anisovich, Yu.M. Shabelski, V.M. Shekhter, *Nucl. Phys. B* **133**, 477
(1978).

[19] S. Eremin, S. Voloshin, *Phys. Rev. C* **67**, 064905 (2003)
[`arXiv:nucl-th/0302071`].

[20] P. Kumar Netrakanti, B. Mohanty, *Phys. Rev. C* **70**, 027901 (2004)
[`arXiv:nucl-ex/0401036`].

[21] A. Białas, A. Bzdak, *Phys. Lett. B* **649**, 263 (2007)
[`arXiv:nucl-th/0611021`].

[22] A. Białas, A. Bzdak, *Phys. Rev. C* **77**, 034908 (2008)
[`arXiv:0707.3720 [hep-ph]`].

[23] B. Alver, M. Baker, C. Loizides, P. Steinberg, `arXiv:0805.4411 [nucl-ex]`.

[24] G. Agakishiev *et al.* [STAR Collaboration], *Phys. Rev. C* **86**, 014904 (2012)
[`arXiv:1111.5637 [nucl-ex]`].

[25] S.S. Adler *et al.* [PHENIX Collaboration], *Phys. Rev. C* **89**, 044905 (2014)
[`arXiv:1312.6676 [nucl-ex]`].

[26] C. Loizides, J. Nagle, P. Steinberg, *SoftwareX* **1–2**, 13 (2015)
[`arXiv:1408.2549 [nucl-ex]`].

[27] A. Adare *et al.* [PHENIX Collaboration], *Phys. Rev. C* **93**, 024901 (2016)
[`arXiv:1509.06727 [nucl-ex]`].

[28] R.A. Lacey *et al.*, *Universe* **4**, 22 (2018) [`arXiv:1601.06001 [nucl-ex]`].

[29] P. Bożek, W. Broniowski, M. Rybczyński, *Phys. Rev. C* **94**, 014902 (2016) [arXiv:1604.07697 [nucl-th]].

[30] L. Zheng, Z. Yin, *Eur. Phys. J. A* **52**, 45 (2016) [arXiv:1603.02515 [nucl-th]].

[31] E.K.G. Sarkisyan, A.N. Mishra, R. Sahoo, A.S. Sakharov, *Phys. Rev. D* **94**, 011501 (2016) [arXiv:1603.09040 [hep-ph]].

[32] J.T. Mitchell, D.V. Perepelitsa, M.J. Tannenbaum, P.W. Stankus, *Phys. Rev. C* **93**, 054910 (2016) [arXiv:1603.08836 [nucl-ex]].

[33] O.S.K. Chaturvedi, P.K. Srivastava, A. Kumar, B.K. Singh, *Eur. Phys. J. Plus* **131**, 438 (2016) [arXiv:1606.08956 [hep-ph]].

[34] C. Loizides, *Phys. Rev. C* **94**, 024914 (2016) [arXiv:1603.07375 [nucl-ex]].

[35] M.J. Tannenbaum, *Mod. Phys. Lett. A* **33**, 1830001 (2017) [arXiv:1801.06063 [nucl-ex]].

[36] A. Białas, W. Czyż, *Acta Phys. Pol. B* **36**, 905 (2005) [arXiv:hep-ph/0410265].

[37] M. Barej, A. Bzdak, P. Gutowski, *Phys. Rev. C* **97**, 034901 (2018) [arXiv:1712.02618 [hep-ph]].

[38] A. Adare *et al.* [PHENIX Collaboration], *Phys. Rev. Lett.* **121**, 222301 (2018) [arXiv:1807.11928 [nucl-ex]].

[39] A. Adil, M. Gyulassy, T. Hirano, *Phys. Rev. D* **73**, 074006 (2006) [arXiv:nucl-th/0509064].

[40] P. Bożek, I. Wyskiel, *Phys. Rev. C* **81**, 054902 (2010) [arXiv:1002.4999 [nucl-th]].

[41] P. Bożek, W. Broniowski, *Phys. Rev. C* **88**, 014903 (2013) [arXiv:1304.3044 [nucl-th]].

[42] A. Monnai, B. Schenke, *Phys. Lett. B* **752**, 317 (2016) [arXiv:1509.04103 [nucl-th]].

[43] S. Chatterjee, P. Bożek, *Phys. Rev. C* **96**, 014906 (2017) [arXiv:1704.02777 [nucl-th]].

[44] B.B. Back *et al.* [PHOBOS Collaboration], *Phys. Rev. Lett.* **93**, 082301 (2004) [arXiv:nucl-ex/0311009].

[45] B.B. Back *et al.* [PHOBOS Collaboration], *Phys. Rev. C* **72**, 031901 (2005) [arXiv:nucl-ex/0409021].

[46] B.B. Back *et al.*, *Phys. Rev. Lett.* **91**, 052303 (2003) [arXiv:nucl-ex/0210015].

[47] M. Rybczyński, G. Stefanek, W. Broniowski, P. Bożek, *Comput. Phys. Commun.* **185**, 1759 (2014) [arXiv:1310.5475 [nucl-th]].

[48] S.J. Brodsky, J.F. Gunion, J.H. Kuhn, *Phys. Rev. Lett.* **39**, 1120 (1977).

[49] A. Bzdak, D. Teaney, *Phys. Rev. C* **87**, 024906 (2013) [arXiv:1210.1965 [nucl-th]].

[50] G. Aad *et al.* [ATLAS Collaboration], ATLAS-CONF-2015-020.

[51] G. Aad *et al.* [ATLAS Collaboration], ATLAS-CONF-2015-051.